

Excitation and Fragment-Neutron Correlations of Halo Nuclei ^{B,G}

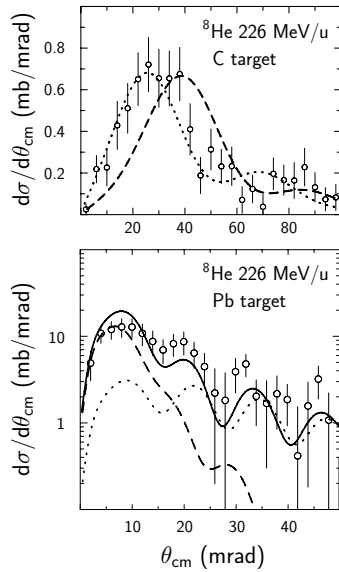
D. Aleksandrov¹, T. Aumann², L. Axelsson³, T. Baumann², M.J.G. Borge⁴, D. Cortina-Gil², L.V. Chulkov^{1,2}, W. Dostal⁵, B. Eberlein^{5,2}, Th.W. Elze⁶, H. Emling², C. Forssén³, H. Geissel², A. Grünschloß⁶, M. Hellström², B. Jonson³, J.V. Kratz⁵, R. Kulessa⁷, Y. Leifels², A. Leistenschneider⁶, K. Markenroth³, M. Meister^{3,8}, I. Mukha^{1,8}, G. Münzenberg², T. Nilsson³, G. Nyman³, M. Pfützner², A. Richter⁸, K. Riisager⁹, C. Scheidenberger², G. Schrieder⁸, H. Simon⁸, O. Tengblad⁴, M.V. Zhukov³

¹Kurchatov Institute, Moscow, ²GSi Darmstadt, ³CTH Göteborg, ⁴CSIC Madrid, ⁵Univ. Mainz, ⁶Univ. Frankfurt, ⁷Univ. Kraków, ⁸TU Darmstadt, ⁹Univ. Aarhus,

Dissociation of ⁸He and ¹⁴Be in carbon and lead targets has been studied in kinematically complete experiments. The data allow to deduce invariant mass spectra, angular distributions in the one neutron knock-out channel as well as inelastic scattering in the 2n decay channels.

The invariant mass spectrum in the inelastic channel ⁶He+n+n shows a broad distribution extending up to about 3.5 MeV. This may be interpreted either (i) as a single broad 1⁻ resonance or (ii) as a relatively narrow 2⁺ state and a broad peak from higher excited 1⁻ state.

Figure 1: Differential cross section for inelastic scattering of ⁸He on two different targets. C target (top): experimental data are compared with DWBA calculations for dipole (dotted line) and quadrupole (dashed line) excitations. Pb target (bottom): the contribution from the electromagnetic dissociation is shown as dashed line while the nuclear diffractive dissociation is displayed as dotted lines. The calculations where performed in eikonal DWBA and result in the solid line as sum of the two processes.



The dominance of dipole transitions can be seen in Figure 1 (top) where the experimental angular distribution for ⁸He inelastic scattering on a carbon target [1] is shown in comparison with DWBA calculations. The differential cross section obtained for ⁸He inelastic scattering from a lead target shown in Fig. 1 (bottom) exhibits Coulomb-nuclear interferences, thus confirming the $J^\pi = 1^-$ assignment to a broad peak in the ⁸He invariant-mass spectrum.

Table 1 presents partial cross sections for the ⁸He fragmentation on carbon and lead targets. In both cases, neutron knock-out is the dominating reaction channel. It becomes comparable in magnitude with the inelastic scattering in case of the ²⁰⁸Pb target. For the carbon target, the difference of the ⁸He and ⁴He interaction cross sections exceeds the sum $\sigma_{in} + \sigma_{-1n} + \sigma_{-2n}$ in ⁸He by about 100 mb. This excess is due to the breakup into $\alpha+4n$ and is likely a sign of the five-body character of ⁸He.

For the lead target, the difference of the ⁸He and ⁴He interaction cross sections is smaller than the sum $\sigma_{in} + \sigma_{-1n} + \sigma_{-2n}$. The Coulomb dissociation cross section can be calculated from this difference by taking

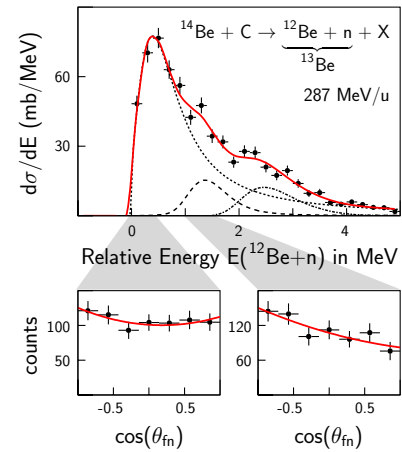
into account the missing contribution of about 250 mb from the breakup into $\alpha+4n$. An independent method based on DWBA calculations and a normalisation to the experimental angular distribution at forward angles gave the same result. The contribution of electromagnetic dissociation is then 160 mb which leads to a $B(E1)$ value equal to $0.46 e^2 fm^2$ below 7 MeV excitation energy.

Table 1: Extracted contributions of nuclear (N) and electromagnetic (C) processes to the fragmentation cross sections of ⁸He on lead and on carbon targets. Here σ_{in} denotes cross sections for inelastic scattering, whereas σ_{-1n} corresponds to one-neutron knock-out.

Target	σ_{in}^N (mb)	σ_{in}^C (mb)	σ_{-1n}^N (mb)	σ_{-1n}^C (mb)
Lead	80 ± 12	160 ± 25	322 ± 37	6 ± 97
Carbon	32 ± 5		129 ± 15	

The structure of the unbound ¹³Be is currently poorly understood. The ¹²Be-n relative energy spectrum shown in Figure 2 and obtained in a one-neutron knockout reaction of ¹⁴Be on a carbon target, reveals interesting structures. The angular distributions analysed as explained in [2], but gated on different bins in the relative energy spectrum show isotropy (bottom, left) and asymmetry (bottom, right) as expected for adopted s- and p- wave resonances at about 250 keV and 1.2 MeV, respectively.

Figure 2: (Top) The relative energy spectrum between ¹²Be fragments and neutrons. The solid line represents a fit to the data taking s (dotted), p (dashed) and d (dashed dotted) contributions into account. (Bottom) angular distributions gated on the relative energy as indicated by the shaded areas. The solid lines are fits with 2nd order polynomials to guide the eye.



The asymmetric distribution stems hereby from the interference of two overlapping states with different parity. As the groundstate shows the typical behaviour of an s-intruder state, the interfering first excited state should be a p-state. This allows a tentative assignment of ($1s_{1/2}$), ($0p_{1/2}$) and ($0d_{5/2}$) for the groundstate and the first two excited states of ¹³Be.

References

- [1] K. Markenroth et al., Nucl. Phys. **A679** (2001) 462
- [2] H. Simon et al., Phys. Rev. Lett. **83** (1999) 469